LASER HEATER TRANSVERSE SHAPING TO IMPROVE MICROBUNCHING SUPRRESSION FOR X-RAY FELS

S. Li*, A. Fry, S. Gilevich, Z. Huang, A. Marinelli, D. Ratner, J. Robinson
SLAC, Menlo Park, CA 94025, USA

Abstract

In X-ray free electron lasers (FELs), a small amount of initial density or energy modulation in the electron beam can be amplified through the acceleration and bunch compression process. The undesired microbunching on the electron bunch will increase slice energy spread and degrade the FEL performance. The Linac Coherent Light Source (LCLS) laser heater (LH) system was installed to increase the uncorrelated energy spread in the electron beam in order to suppress the microbunching instability. The distribution of the induced energy spread depends strongly on the transverse profile of the heater laser and has a large effect on microbunching suppression. In this paper, we present theoretical calculations for the LH induced energy spread and discuss strategies to shape the laser profile in order to obtain better suppression of microbunching. We present analysis and potential methods to achieve Gaussian and Gaussian-like energy spread on the electron beam.

INTRODUCTION

At the Linear Coherent Light Source (LCLS), the laser heater (LH) system was installed in the injector area to suppress the microbunching instability by increasing the uncorrelated energy spread [1, 2]. The interaction between the heater laser and the electron beam takes place in a short undulator and gives rise to an energy modulation on the electron beam. The distribution of the laser-heater-induced energy spread affects the suppression of the microbunching instability. The energy modulation amplitude each electron experiences varies depending on the location of the electron relative to the laser transverse profile. Therefore one can control the energy spread distribution by transversely shaping the heater laser profile, and hence improve the suppression of microbunching instability.

In this paper we present theoretical calculations to relate the laser transverse profile with laser-heater-induced energy spread distribution. We discuss two methods of generating Gaussian-like energy spread using a fundamental Gaussian mode and a Laguerre-Gaussian (LG) mode, and compare their microbunching suppression effect and power efficiency. Lastly, we investigate the possibility of implementing a Gaussian speckle distribution, an approach independent of the transverse electron distribution.

* siqili@slac.stanford.edu

LASER HEATER SUPPRESSION THEORY

The energy modulation induced by laser-electron interaction is obtained in [1],

$$\delta_L(r) = \sqrt{\frac{P_L}{P_0}}\frac{KL_u}{\gamma_0\sigma_r}\left[J_0[\frac{K^2}{4+2K^2}] - J_1[\frac{K^2}{4+2K^2}]\right] f(r) \equiv Af(r), \tag{1}$$

where P_L is the peak laser power, $P_0 = I_A mc^2/e \approx 8.7\text{GW}$, K is the undulator strength parameter, γ_0 is the relativistic factor of electron beam energy, L_u is undulator period, σ_r is the rms spot size of the laser, $J_{0,1}$ are the Bessel functions, r is the radial position of the electron, and $f(r)$ describes any arbitrary transverse profile of the laser beam. On the right hand side of the equation, we group the constants in front of the laser profile $f(r)$ into one constant A.

If we assume a Gaussian electron distribution and integrate the energy-modulated electron beam in transverse and longitudinal coordinates, we get the expression for the modified energy distribution,

$$\begin{aligned} V(\delta) &= \frac{1}{\pi\sigma_x^2\sqrt{2\pi}\sigma_{\delta0}}\int r dr d\xi \frac{e^{-\frac{r^2}{2\sigma_x^2}-\frac{\xi^2}{2\sigma_{\delta0}^2}}}{\sqrt{\delta_L(r)^2-(\delta-\xi)^2}} \\ &\approx \int \frac{1}{\pi\sigma_x^2} r\, dr\, e^{-\frac{r^2}{2\sigma_x^2}} \frac{1}{\sqrt{\delta_L(r)^2-\delta^2}}, \end{aligned} \tag{2}$$

where σ_x is the rms size of the electron beam, and $\sigma_{\delta0}$ is the initial energy spread in the electron beam. $\sigma_{\delta0}$ is typically 1 to 3 keV, and is relatively small compared to the induced energy spread which will be shown below to be around a few tens of keV. Thus we ignore its contribution in the last line of Eq. (2) and throughout the rest of this paper.

The microbunching gain is defined as the ratio of the final bunching factor to the initial bunching factor $\left|\frac{b_f}{b_0}\right|$, which can be approximated as [1]

$$G \approx \frac{I_0}{\gamma I_A}\left|k_f R_{56}\int_0^L ds \frac{4\pi Z(k_0;s)}{Z_0}\right| S_L(k_f R_{56} A, \frac{\sigma_r}{\sigma_x}), \tag{3}$$

where I_0 is the peak current, I_A is the Alfven current, $k_f = Ck_0$ is the compressed modulation wave number through compression C, $Z(k;s)$ is the longitudinal space charge impedance defined below (Eq. (4)), and S_L is the gain suppression factor defined as the Fourier transform of $V(\delta)$. The impedance function is

$$Z(k,s) = \frac{iZ_0}{\pi k r_b^2}\left[1 - \frac{kr_b}{\gamma}K_1\left(\frac{kr_b}{\gamma}\right)\right], \tag{4}$$

ISBN 978-3-95450-134-2

where r_b is the radius of the transverse cross section for a uniform distribution. In the following, we take $r_b \approx 2\sigma_x$. The suppression factor is

$$S_L(kR_{56}A, B) = \int R\,dR\,e^{-\frac{R^2}{2}} J_0[kR_{56}Af(r)]\,, \qquad (5)$$

with

$$R \equiv \frac{r}{\sigma_x},\, B \equiv \frac{\sigma_r}{\sigma_x}\,. \qquad (6)$$

To get a desired Gaussian energy distribution $V(\delta)$, we need a Gaussian suppression factor S_L because they are related to each other by Fourier transform. Note that for a Gaussian transverse electron distribution, a linear R dependence of the laser profile will generate a perfect Gaussian suppression factor, hence a Gaussian energy distribution:

$$S_L(A') = \int_0^\infty R\,dR\,e^{-\frac{R^2}{2}} J_0(A'R) = e^{-A'^2/2}, \qquad (7)$$

where $A' \equiv kR_{56}A$ and k and R_{56} are kept fixed.

At the end of compression, the gain becomes

$$G \approx \frac{I_0}{\gamma I_A}\left|k_f R_{56} L \frac{4\pi Z(k_f)}{Z_0}\right| S_L(k_f R_{56} A, \frac{\sigma_r}{\sigma_x})\,. \qquad (8)$$

Again, we use the approximation that $\sigma_{\delta 0}$ is negligible compared to the induced energy spread in the above equation. The variance of current profile is proportional to $\int_0^\infty dk_0 |G(k_0) b_0(k_0)|^2$ [1]. In the approximation of $b_0(k_0)$ being the white noise and independent of wave length, we can use the following integral as a measure of how well the laser heater suppresses the microbunching gain

$$I = \int_0^\infty G^2(k_0) dk_0\,. \qquad (9)$$

The smaller I, the better the laser heater suppresses the microbunching gain. In the following analysis, we will use the I integral to compare the different methods of generating a desired energy spread distribution.

Note that in Eq. (5) the suppression factor is defined in terms of the energy modulation amplitude A, whereas the FEL performance is evaluated in terms of the rms energy spread. We would like to compare microbunching suppression of different laser profiles with the same induced rms energy spread. By definition, the square of rms energy spread is $\sigma_\delta^2 = \int \delta^2 V(\delta)\,d\delta$, where $V(\delta)$ also depends on δ_L. We get

$$\sigma_\delta = A\sqrt{\int_0^\infty \frac{r\,dr}{2\sigma_x^2} e^{-\frac{r^2}{2\sigma_x^2}} f^2(r)}. \qquad (10)$$

Therefore we can convert between energy modulation amplitude and rms induced energy spread using the factor in Eq. (10) for any radially symmetric laser profile $f(r)$.

TWO EXAMPLES: FUNDAMENTAL GAUSSIAN MODE AND LAGUERRE-GAUSSIAN MODE

There are several methods to generate a perfectly Gaussian or Gaussian-like energy spread by manipulating the laser heater transverse profile. Here in this section, we go through two examples. In the analysis in this section, the beam goes through one linac (L1) and one bunch compressor (BC1) with the following parameters:

Table 1: Simulation Parameters

Parameter	Value
R_{56}	45 mm
r_b	300 μ m
Peak current I_0	30 A
γ	489
L1 length L	12 m
σ_δ	15 keV
BC1 compression C_1	7

Fundamental Gaussian Laser Mode

We can now plug in specific laser profiles to the theories in the above section. Let's start with a fundamental Gaussian mode laser,

$$\delta_L(r) = Ae^{-\frac{r^2}{4\sigma_r^2}} = Ae^{-\frac{R^2}{4B_G{}^2}}\,, \qquad (11)$$

with $B_G = \frac{\sigma_r}{\sigma_x}$ as in Eq. (6). The subscript G denotes Gaussian mode. Plugging Eq. (11) into Eq. (10), we get $A = \sqrt{2(1+\frac{1}{B_G^2})}\sigma_\delta$, consistent with [2].

We can calculate the suppression factor and gain, which will give us the I integral as a function of B_G. Physically, this tells us the suppression effect as a function of the laser size relative to the electron beam size. Figure 1 shows that the best suppression occurs at $B_G = 0.9$. As we move away from $B_G = 0.9$ in either direction, the I integral starts to increase, suggesting we should operate in the range of $0.8 < B_G < 1.2$. We refer to the case when $B_G = 1$ as "matched Gaussian" or MG.

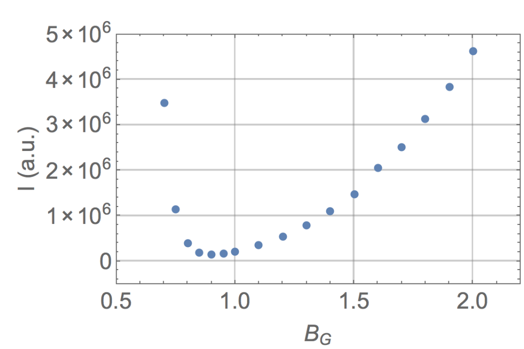

Figure 1: Gaussian laser profile suppression integral I as a function of B_G.

Laguerre-Guassian Laser Mode

We have shown that a linear R dependence of the laser profile produces a perfectly Gaussian energy spread (Eq. (7)).

ISBN 978-3-95450-134-2

One way to approach the linear R dependence is to use the first order Laguerre-Gaussian (LG_0^1) mode,

$$\delta_L(r) = ARe^{-\frac{R^2}{2B_{LG}^2}}, \tag{12}$$

again with $B_{LG} = \frac{\sigma_r}{\sigma_x}$ as in Eq. (6). Note by the above definition of LG_0^1 mode, the σ_r in the equation is the same as the rms laser beam size. When B_{LG} is large, the electron sees a linearly increasing energy modulation as it moves from the center to the edge on the transverse plane. Following the same procedure as in the previous section, we can find the normalization factor $A = (1 + \frac{2}{B_{LG}^2})\sigma_\delta$. Similarly, from suppression factor and gain, we can get I integral as a function of B_{LG} (Fig. 2). The horizontal line refers to the suppression due to matched Gaussian laser profile. When $B_{LG} = 3$, the LG mode is better than a matched Gaussian by a factor of 3. As B_{LG} reaches 3.5, the I integral starts to flatten, making it meaningless to further increase B_{LG}. At the current LCLS laser heater, the Gaussian laser profile has approximately $B_G = 1.5$. In this case, the LG mode with $B_{LG} = 3$ improves over the Gaussian profile by a factor of 23 in terms of the I integral.

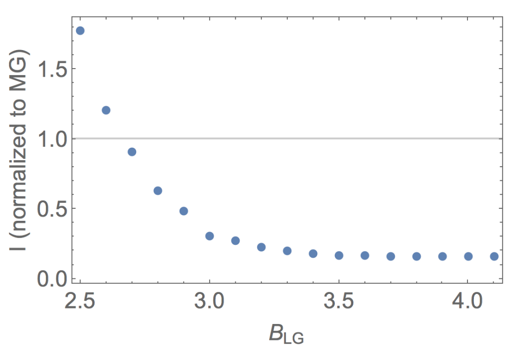

Figure 2: LG laser profile suppression integral I as a function of B_{LG}. The horizontal line corresponds to the integral I for matched Gaussian laser profile.

To produce an LG mode at LCLS, we can use a liquid crystal spatial light modulator (SLM) to convert the existing Gaussian mode to the helical LG mode by phase modulation. The LG_0^1 mode requires a helical phase pattern linearly dependent on azimuthal angle ϕ and independent of radial position r. We can control the output beam size by adding a blazed phase pattern to the helical phase pattern with a defined aperture. Matsumoto et. al. in [3] present the detailed procedure of phase compensation and demonstrate efficient conversion of Gaussian beam to higher-order LG modes.

Comparison

To compare the Gaussian mode and LG mode, we can use the suppression factor and the final energy spread as a metric to measure which one suppresses microbunching better.

Figure 3 shows the suppression factor S_L as a function of modulation wavenumber k for different laser profiles. $B_{LG} = 10$ resembles the linear R dependence profile that produces a Gaussian suppression factor. $B_{LG} = 3$ shows oscillatory behaviors deviating away from a smooth Gaussian. With smaller B_{LG} the oscillation becomes more obvious. The matched Gaussian case shows a stronger oscillation than $B_{LG} = 3$. The current LCLS operation ($B_G = 1.5$) shows the strongest oscillation among the curves.

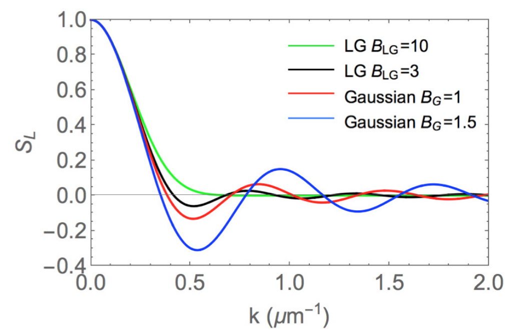

Figure 3: Suppression factor S_L as a function of modulation wavenumber k.

A more quantitative way of comparison is the FEL final energy spread. The simulation takes in analytical expression for the suppression factor, so we compare the Gaussian profiles with several B_G values with a linear R dependence laser profile. In this simulation, we take initial energy spread to be 1 keV, final beam energy 4.3 GeV. As shown by Fig. 4, the linear R dependence profile reduces final SES by 25% compared to matched Gaussian mode. Compared to Gaussian profile with $B_G = 1.5$, the linear R dependence profile improves the final SES by 66%. The result indicates that if we could produce a sufficiently Gaussian-like energy spread, the final energy spread will be improved significantly.

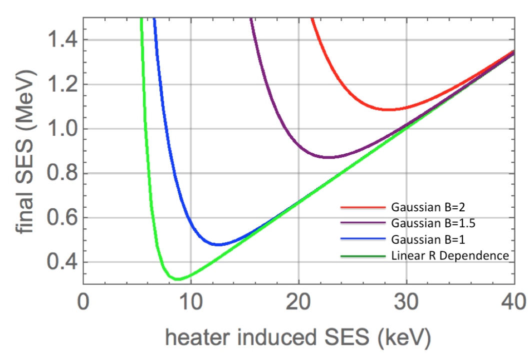

Figure 4: Final slice energy spread (SES) as a function of heater induced SES.

Another important consideration is power efficiency. We would like to compare the ratio of averaged induced energy modulation to power for both LG mode and Gaussian mode. In Eq. (13) we ignore the normalization factors because they cancel as we consider the ratio.

$$\left(\frac{\langle\delta^2\rangle}{P}\right)_{MG} \Big/ \left(\frac{\langle\delta^2\rangle}{P}\right)_{LG} = \frac{(2 + B_{LG}^2)^2}{4(1 + B_G^2)}, \tag{13}$$

ISBN 978-3-95450-134-2

Table 2 illustrates the efficiency ratio to achieve same energy spread for various values of B_G and B_{LG}. This is a theoretical calculation. Additional power loss comes from converting a Gaussian mode to LG mode, and the spatial modulator efficiency.

Table 2: Efficiency ratio for different B_G and B_{LG}

B_G	B_{LG}	$P_{LG}/P_{Gaussian}$
1	3	15
1	4	41
1.5	3	9
1.5	4	25
2	3	6
2	4	16

SPECKLE PATTERN

One drawback of the above schemes is that they require careful measurement of the beam size (matched Gaussian) or beam distribution (LG mode). An alternative approach is to create a speckle pattern so that different electrons see different modulation amplitudes. By modulating with a single frequency laser of wavenumber k and transversely varying amplitude $A(x, y)sin(kz)$, an electron receives an energy modulation, δ, with a probability distribution $P(\delta)$ determined by the laser profile, $A(x, y)$. The expected modulation is given by

$$P(\delta) = \int_{\delta}^{\infty} Q(\eta)R(\eta,\delta)d\eta, \tag{14}$$

where $Q(\eta)$ is the probability that an electron interacts with a transverse laser field of amplitude $A(x, y) = \eta$, and $R(\eta,\delta)$ is the probability that a field $\eta \sin(kz)$ produces a modulation of amplitude δ (due to the sinusoidal variation in time). The interpretation of $R(\eta,\delta)$ is the probability density function of a sine wave, $R(\eta,\delta) = 2/(\pi\eta\sqrt{1-\delta^2/\eta^2})$ (where we have normalized so that $\int_0^{\eta} R d\delta = 1$). Note that $R(\eta,\delta) = 0$ for $\eta < \delta$, so the lower limit of the integral is δ.

Choosing an appropriate intensity distribution $Q(\eta)$ will give a Gaussian energy spread independent of the electron distribution. With

$$Q(\eta) = \frac{\eta}{\sigma_r^2} e^{-\eta^2/2\sigma_r^2}, \tag{15}$$

we find a Gaussian energy distribution

$$P(\delta) = \frac{2}{\pi\sigma_r^2}\int_{\delta}^{\infty} d\eta \frac{\eta e^{-\eta^2/2\sigma_r^2}}{\sqrt{\eta^2-\delta^2}} = \sqrt{\frac{2}{\pi\sigma_r^2}} e^{-\delta^2/2\sigma_r^2}. \tag{16}$$

As for the LG mode, a spatial modulator can also produce an approximate intensity distribution given by $Q(\eta)$. To minimize the effect of transverse smearing of both electrons and laser, we group the pixels by intensity. Each block of pixels have intensities given by $Q(\eta)$, and we repeat the block throughout the transverse plane, requiring the block feature small compared to the electron rms beam size (Fig. 5). We then find a Gaussian-like energy distribution regardless of the electron beam's transverse distribution, as shown in Fig. 6.

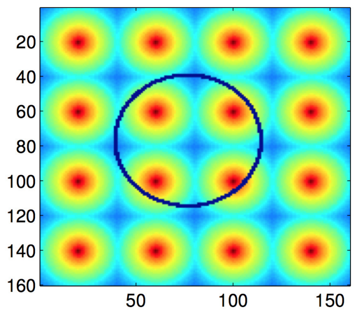

Figure 5: An example of speckle pattern with the blue ring representing the FWHM of a Gaussian electron beam with a random offset.

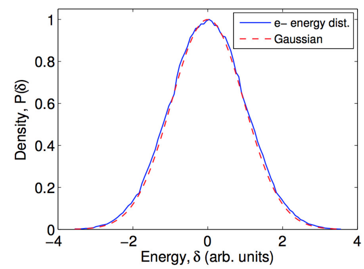

Figure 6: Electron energy distribution produced by the speckle pattern shown in Fig. 5.

The speckle approach assumes that the pattern is maintained throughout the undulator length in the LCLS LH system, i.e. the undulator length L_u must be shorter than the confocal parameter $b = 2\pi w_0^2/\lambda$, with smallest feature size w_0 and wavelength λ. For the current LCLS LH design, the confocal parameter, $b \sim 2$ cm, is much to small for the beam to maintain imaging, and implementing this approach would require new hardware. However, if designing a laser heater system from scratch, it should be possible to accommodate a sufficiently long confocal parameter; for example, using the LCLS cathode laser ($\lambda = 260$ nm), $\sigma_r = 300\,\mu$m, and $w_0 = 100\,\mu$m, gives a reasonable confocal parameter of $b = 0.25$ m.

CONCLUSION

In this paper, we have presented the theoretical background of the effect of transverse laser profile on the electron beam energy spread in the LCLS LH system. In particular, we have shown that a linear R dependence in the laser profile generates a perfectly Gaussian energy spread. As examples, we considered the fundamental Gaussian mode and the Laguerre-Gaussian mode laser, to generate a Gaussian-

ISBN 978-3-95450-134-2

like energy spread. For the fundamental Gaussian mode, our analysis is consistent with the result in [1] that a matched Gaussian laser is optimal in terms of suppressing the microbunching instability. With LG mode we are able to achieve even better suppression of microbunching when the rms laser beam size is larger than the rms electron beam size. The challenge lies in implementing LG mode with reasonable efficiency. We also investigated the possibility of generating a Gaussian energy spread with a speckle pattern by enforcing an intensity distribution (Eq. (15)) on a spatial modulator. This method has an advantage of being resistant to transverse motion and overlap, but proves difficult with the current LCLS laser heater setup.

REFERENCES

[1] Huang, Zhirong, et al. "Suppression of microbunching instability in the linac coherent light source." *Physical Review Special Topics-Accelerators and Beams* 7.7 (2004): 074401.

[2] Huang, Zhirong, et al. "Measurements of the linac coherent light source laser heater and its impact on the x-ray free-electron laser performance." *Physical Review Special Topics-Accelerators and Beams* 13.2 (2010): 020703.

[3] Matsumoto, Naoya, et al. "Generation of high-quality higher-order Laguerre-Gaussian beams using liquid-crystal-on-silicon spatial light modulators." *JOSA A* 25.7 (2008): 1642-1651.

ISBN 978-3-95450-134-2